

Module 3 - Attenuation in Optical Fibers



Dr. B.G. Potter

Professor, Material Science and Engineering Dept, University of Arizona

Dr. B.G.Potter is a Professor of Material Science and Engineering in the University of Arizona. Research activity within Dr. Potter's group is centered on the synthesis and study of glass, ceramic, and molecular hybrid materials for photonic and electronic applications. Active research and ongoing programs include: optically driven molecular assembly strategies, nanostructured photovoltaic energy conversion materials, photoactivated phenomena in glass and hybrid thin films, solution and physical vapor phase deposition of thin films and nanocomposites (oxides, inorganic-organic hybrids), thermal stability of complex oxide optical materials, environmental sensing, optical behavior of rare-earth-doped matrices, semiconductor quantum-dot ensembles, and optical spectroscopy.

Email: bgpotter@mse.arizona.edu

Introduction

Efficient transmission of light at the operational wavelength(s) is the primary function of fiber optics needed for a range of applications (e.g. long-haul telecommunications, fiber lasers, optical delivery for surgical or biomedical applications). Reduction in the intensity of light as it propagates within the fiber is called “attenuation”. The finite attenuation present in any optical fiber requires that fiber system design address degradation in signal strength through such approaches as signal amplification, interconnect optimization, fiber geometry design, and environmental isolation. An understanding of attenuation mechanisms and the potential for their minimization is, thus, of great importance in the efficient and economic use of fiber optics.

Any process that results in a reduction in the light intensity measured after propagation through a material contributes to the observed optical attenuation. In principle, all attenuation mechanisms can be traced back to the multilength scale structure of the glass itself (e.g. atomic structure, point defects, second-phase inclusions) or structures arising from the fiberization process and/or optical design of the fiber (e.g. interfacial structure at the core-clad interface, uniformity of core-clad structure along fiber length). Thus, the control of material structure (through composition, material processing, and fiber fabrication controls) is the primary means to reduce attenuation in

the finished fiber. An understanding, however, of the underlying optical phenomena at work and their relationship to material composition and structure is needed.

The overall optical throughput (transmission) of an optical fiber can be quantified in terms of the input optical power, $P(0)$, and the output power, $P(z)$ observed after light propagates a distance, z , along the fiber length:

$$P(z) = P(0)e^{-\alpha_{total}z} \quad (\text{Equation 3.1})$$

and

$$\%T = \frac{P(z)}{P(0)} \quad (\text{Equation 3.2})$$

where: α_{total} = the total attenuation coefficient (i.e. involving all contributions to attenuation); %T is the percentage optical power transmission. **Equation 3.1** is referred to as Beer's Law and shows that transmitted power decreases exponentially with propagation distance through the fiber.

In an optical fiber transmission context, the attenuation coefficient above is often expressed in base-10 form:

$$\alpha_{total} (\text{dB/km}) = \frac{10}{z} \log \left[\frac{P(0)}{P(z)} \right] = 4.343\alpha_{total} (\text{km}^{-1}) \quad (\text{Equation 3.3})$$

This final parameter is often referred to as the "fiber loss".

It is important to note at the outset, that %T is an extrinsic measure of the fibers ability to transmit optical power. Multiple contributions to an overall transmission value arise from intrinsic fiber material properties as well as attenuation mechanisms associated with fiber fabrication (preform development, drawing conditions). These different processes add to the observed reduction in transmitted power ($P(z)$) through contributions to the magnitude and wavelength dependence of α_{total} .

The present module will provide an overview of the origins of optical signal attenuation in fiber optics. Optical phenomena contributing to attenuation that arise from materials-related mechanisms within the fiber will serve as the primary focus. Potential attenuation sources associated with fiber system design (e.g. interconnection, cabling, environmental effects etc.) will also be briefly introduced.

3.1 Optical Absorption

Optical absorption involves the direct transfer of energy from the propagating light beam to the material structure, resulting in the excitation of the material to a higher energy state. This concept was previously examined in Module 1 in which the material was described in terms of a collection of oscillators, each available to absorb energy from an optical field oscillating at a frequency that is equal (or nearly equal) to the fundamental resonance frequency of given oscillator. The energy absorption promotes the oscillator to a higher energy level. This resonance condition is directly observed in the dispersion (frequency dependent) behavior of the complex dielectric function for the material which, in turn, gives rise to the complex refractive index at optical frequencies.

More specifically, the propagation of light within a material can be described in terms of a complex refractive index (n^*):

$$n^* = n(\omega) + i\kappa(\omega) \quad (\text{Equation 3.4})$$

where: $n(\omega)$ = real portion of the refractive index; $\kappa(\omega)$ = extinction coefficient.

and:

$$\alpha(\omega) = \frac{2\omega\kappa}{c}. \quad (\text{Equation 3.5})$$

where: $\alpha(\omega)$ = absorption coefficient; c = speed of light.

Thus, via equation (3.1), the absorption coefficient contributes directly to the output power observed through its participation in the overall attenuation coefficient, α_{total} .

In terms of the oscillator picture of a material, different structural elements will each contribute to the overall magnitude, and frequency dependence, of the optical absorption. Thus, the material composition and specific structural characteristics will directly impact the optical absorption observed at a particular wavelength of light. Some general contributions to optical absorption in fiber optic glasses are provided below:

Intrinsic absorption: Base Glass

The intrinsic optical absorption responses of core and clad glasses used were previously discussed as the primary factor dictating the transmission window (and ultimately the operational wavelengths) for an optical fiber. In the present context, the transmission window is defined by

the spectral region bounded by the high optical absorption arising from electronic transitions across the band-gap of the material (higher energy absorption edge) and the excitation of vibrational motion of the extended glass network and more localized structural features (lower energy absorption edge). The high transmission spectral band that lies between these two absorption edges is often referred to as a “forbidden gap” referring to an absence of allowed energy states supporting energy absorption in this spectral range so that optical transparency is observed.

The frequency dependence of α at the absorption onsets for both the electronic and vibrational (phonon) processes can be generally described with an exponential function form. For the electronic-transition band-edge, the absorption coefficient is described by the Urbach relationship:

$$\alpha(\omega) = A \exp[\sigma(\hbar\omega - \hbar\omega_o) / kT] \quad (\text{Equation 3.6})$$

where: A , σ , and ω_o are parameters characteristic of the material.

A similar functional dependence of α on frequency for the phonon-based absorption edge (i.e. defining the longer wavelength edge of the transmission window) results in a characteristic wedge shape in the spectral absorption loss characteristic of a particular material. **Figure 3.1** contains a representative spectrum of absorption losses defining the transmission window of a GeO_2 -doped silica glass often used as the core material in telecommunications fibers. Note that α is provided on a log-scale in terms of dB/km. The absorption edge due to electronic transitions across the band-gap for the glass is on the left (higher energies), while the phonon-based absorption edge is to the right (lower energies). Contribution from scattering losses (to be discussed in subsequent sections) are also included.

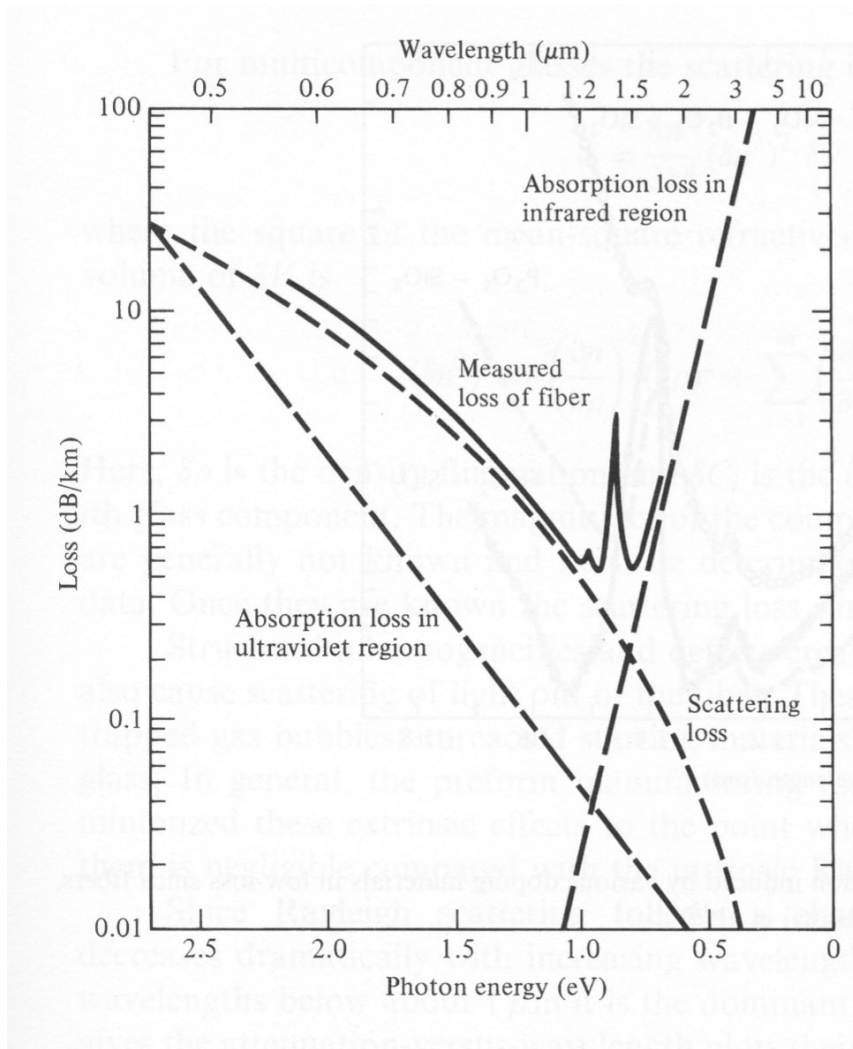


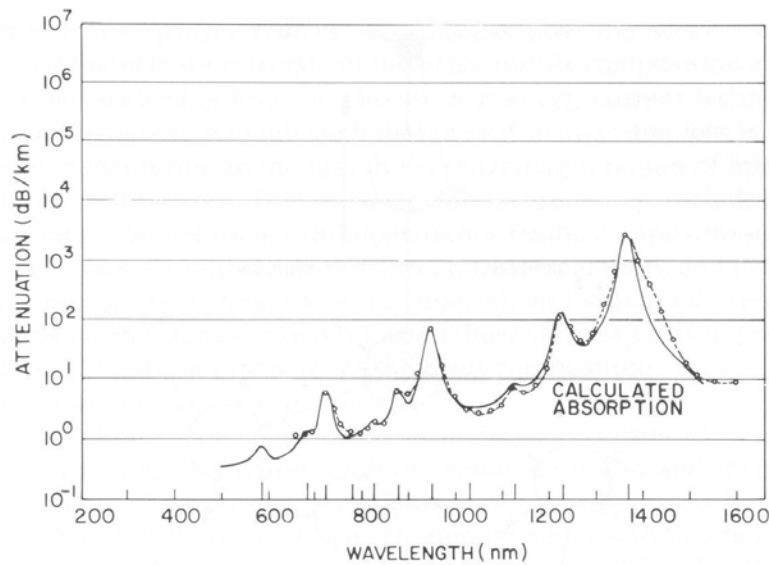
Figure 3.1: Optical fiber attenuation characteristics that bound the transmission window in GeO₂-doped, low-loss, low-OH-content silica fiber.

Of course, the precise frequency dependence (e.g. energy location of these absorption edges) will be dependent upon the glasses used and their specific chemical and structural characteristics. The effect of using heavier atomic constituents in both oxide and nonoxide (e.g. chalcogenide and fluoride) glass systems was previously discussed in Module 1. In this case, the reduction in vibrational energies for these systems produce a significant red-shift in the location of the phonon-edge, resulting in dramatic changes in the spectral regions of transparency for these materials (see Module 1).

Extrinsic absorption processes

In addition to the energy structure of the base glass that defines the transmission window, the presence of defects in the glass structure (e.g. vacancies, over/under coordinated atoms) and/or dopants and impurities can produce localized energy states that exist within the forbidden gap. The presence of such states, thus, enables optical absorption at frequencies within the transmission window. When such absorption processes are at frequencies resonant with the operational wavelength of the fiber, such structural elements present a significant problem in the development of low-loss fiber optic systems.

One of the primary absorbing species common in silica-based glass fibers is water (hydroxyls (OH)) within the glass structure. The fundamental resonances for hydroxyl species, associated with bending and stretching modes of vibration, occur at 2.73 and 6.25 microns, well away from the near-infrared spectral range typically associated with telecommunications wavelengths. While the effect of such absorption processes on attenuation in the near-IR may initially seem minimal, overtones and combination vibrations result in significant absorption well into the near-IR. Table I provides a list of OH-related resonances observed in silica glass (Suprasil) with an OH content of only 1200 ppm. **Figure 3.2** depicts the calculated absorption attenuation for such resonances illustrating the dramatic impact of these effects on fiber transmission behavior. In fact, the sharp peaks at approximately 0.89 and 1.0 eV observed in the low attenuation spectral range of **Figure 3.1** are associated with water-related vibrational absorption.



Calculated absorptive attenuations as a function of wavelength (Keck *et al.*, 1973).

Figure 3.2: *Absorptive attenuation in silicate fiber.*

It was previously discussed in **Modules 1 and 2** that compositional dopants are added to the base silica glass to alter the refractive index of the material. These additions to the glass composition, however, will also influence the electronic and phonon-based absorption observed through

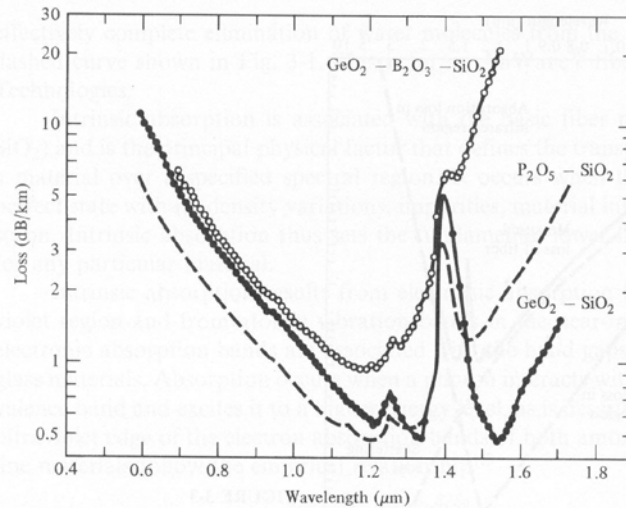
OH Overtones and Combinational Vibrations In Suprasil 1 Vitreous Silica and Their Peak Intensities.^a

Wavelength (μm)	Frequency	Loss (dB/km)
0.60	$5\nu_3^1$	6
0.64	$2\nu_1 + 4\nu_3^1$	1
0.68	$\nu_1 + 4\nu_3^1$	4
0.72	$4\nu_3^1$	70
0.82	$2\nu_1 + 3\nu_3^1$	4
0.88	$\nu_1 + 3\nu_3^1$	90
0.945	$3\nu_3^1$	1,000
1.13	$2\nu_1 + 2\nu_3^1$	110
1.24	$\nu_1 + 2\nu_3^1$	2,800
1.38	$2\nu_3^1$	65,000
1.90	$2\nu_1 + \nu_3^1$	10,300
2.22	$\nu_1 + \nu_3^1$	260,000
2.72	ν_3^1	10,000,000

^a The OH level is about 1200 ppm. From Kaiser (1973).

Table 1

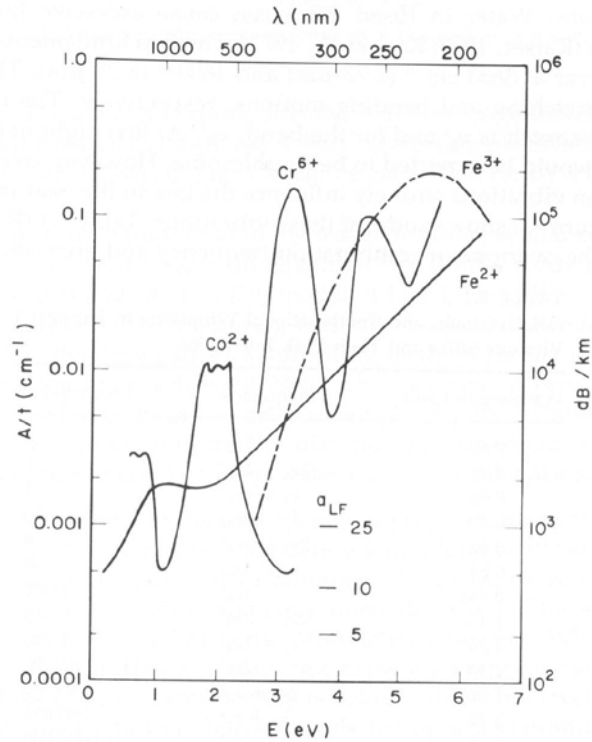
differences in the constituent atomic masses, bond characteristics, and chemistry. **Figure 3.3** compares the effect of common dopants used for refractive index modification in fused silica fibers on the attenuation characteristics of the glass. Note the dramatic impact of dopants on the phonon-edge location and magnitude. Often the type of dopant will also indirectly affect the water content of the glass, through the precursors used for vapor-deposited preform fabrication, producing concomitant changes in the magnitude of OH-related vibrational absorption.



A comparison of the infrared absorption induced by various doping materials in low-loss silica fibers. (Reproduced with permission from Osanai et al.¹³)

Figure 3.3: A comparison of the effects of dopants on infrared absorption in silicate fibers.

Similarly, inadvertent contamination of the glass with metal-ion species, e.g. transition metals (including Fe, Cr, Co), during preform fabrication and/or drawing can also produce marked attenuation in the visible and near-IR spectral ranges. Transitions associated with ligand-field induced transitions within the d-orbital energy level structure of the ions or charge transfer transitions from the metal ion to a coordinating ligand are typically observed. **Figure 3.4** shows a representative attenuation spectrum for transition metal ions in silica. It is precisely this sensitivity to impurities within the glass structure that drove the development of vapor-phase deposition techniques for preform development. Such techniques provide high-purity precursor materials and fabrication methodologies that avoid the potential for contamination associated with conventional melt-and-cast or crucible-draw approaches.



Absorption of some ligand field and charge transfer transitions in glass (Kurkjian and Peterson, 1974).

Figure 3.4: *Representative attenuation spectrum for transition metal ions in silica*

In addition to the influence of dissimilar constituents within the glass, modification in the glass structure associated with missing atoms (vacancies) or disturbances in the anticipated bond topology of the glass network also contribute states within the forbidden band. These states typically result in an extension of absorption into the transparency region (band tail states). Such defect structures often form as the result of thermal processing atmosphere (e.g. redox conditions) or through the stress-induced structural modification (residual strain) produced during fiber drawing. For example, the development of oxygen-deficiencies in germanosilicate glasses results in defect structures (oxygen vacancies in the Ge coordination environment) that produce UV-absorption near the band-edge of the glass. In contrast to deleterious issues associated with optical transparency, selective excitation of these charge-trapping defects has been also associated with the formation of a permanent refractive index change in the near-IR that can be used to produce in-fiber grating structures to impart active optical functionality to the fiber.

3.2 Optical Scattering

In the context of factors contributing to the optical attenuation of light under low intensity conditions (linear optical phenomena), optical scattering is best described in terms of elastic phenomena. In this case, photons interact with spatial variations in material dielectric constant, such that the photons alter their propagation direction, phase, and polarization, without energy loss – i.e. the photon frequency after scattering remains the same, hence the process is called an elastic scattering process. These spatial variations in dielectric constant are usually localized and are called scattering centers. Scattering centers are associated with extrinsic, second phase impurities (including particulate inclusions and bubbles) or intrinsic fluctuations in material density and/or composition.

Using current state-of-the-art silica glass fiber production methods, which largely exclude the formation of extrinsic sources of scattering, intrinsic scattering attenuation effects play the dominant role in telecommunications-grade fiber systems. Primary sources of elastic scattering arise from Rayleigh and Mie scattering in the fiber materials.

Rayleigh Scattering

Rayleigh scattering is dominant when light interacts with scattering centers whose size is much less than the wavelength of the light (typically $\lambda/10$). Even if care is taken to insure that the glass is formed to avoid phase decomposition, e.g. phase separation into two, immiscible glass compositions or crystallization (devitrification), there can still exist local fluctuations in glass density. These fluctuations are formed as the glass is cooled through the glass transition range in that different structural elements of the glass network are frozen at different stages of the cooling process. The explanation for this is simple when it is realized that each structural element in the glass is characterized by a unique, individual structural relaxation time leading to a distribution of structural relaxation times for the bulk material. Such a variation in relaxation rate will result in localized density fluctuations, and Rayleigh scattering, even in very high purity glass.

For a medium with density fluctuations much smaller than the light wavelength, the attenuation coefficient can be given as:

$$\alpha_{Rayleigh} = \frac{8\pi^3}{3\lambda^4} \left(\frac{n_1^2}{n_o^2} - 1 \right)^2 \beta k T_f \quad (\text{Equation 3.7})$$

where: n_1 , n_o = refractive index of the scattering center, medium; β = isothermal compressibility of the medium, k = Boltzman's constant, T_f = the fictive temperature of the glass (corresponding

to the temperature at which density fluctuations are frozen into the glass as it is cooled through the transformation range).

Rayleigh scattering thus exhibits a characteristic $1/\lambda^4$ behavior that favors scattering (and larger attenuation parameters) at shorter wavelengths. Related expressions, incorporating both density and compositional fluctuations for multicomponent glass systems also exhibit the same wavelength dependence. The characteristic scattering loss associated with Rayleigh scattering is contained in **Figure 3.1**.

Mie Scattering

As the size of the scattering center becomes larger, exceeding that valid for a Rayleigh scattering picture of the phenomena and approaching the wavelength of light, the scattering light intensity has a greater angular dependence and the process is governed by Mie scattering theory. For a spherical inclusion with a complex dielectric function given by:

$$\varepsilon^* = \varepsilon_1 + i\varepsilon_2 \quad (\text{Equation 3.8})$$

the attenuation parameter associated with Mie scattering from N spheres/unit volume embedded in a medium with a refractive index of n_o is:

$$\alpha_{Mie} = \frac{18\pi N n_o^3 \varepsilon_2}{\lambda(\varepsilon_1 + 2n_o^2) + \varepsilon_2^2} \quad (\text{Equation 3.9})$$

Typical fluctuations in density or composition at this size scale are associated with phase separation in the glass (i.e. associated with immiscible glass phases) and/or the development of crystallinity. Further increases in scattering center size results in a largely wavelength-independent scattering attenuation behavior, governed by the absorption and reflection behavior at the interfaces involved.

It is important to note that, while conventional oxide (silicate-based) glass fiber systems are relatively free of such phase instabilities, the use of nonoxide glass systems for specialty fiber applications (see Module 1) is often accompanied by decreased phase stability, greater tendency for crystallization, and a greater propensity for environmental attack (water). Moreover, the reliance on melt-and-cast-type preform development with, for example, fluoride glass systems, often increases the probability of extrinsic sources of scattering from contaminant phases and bubbles (see Module 2) both within the volume of the glass and at the core-clad interface.

3.3 Bending Losses

In addition to transmission losses associated with absorption and scattering within the glass components of the optical fiber, the fundamental characteristics of light propagation within the fiber design (i.e. core-clad geometry and index contrast) coupled with the uniformity and control of fiber parameters also present factors contributing to optical loss.

Propagating modes within an optical fiber can be characterized by an electric field distribution with maxima inside the fiber core and evanescent fields that extend outside the fiber core into the cladding **Figure 3.5**. Thus, some of the optical energy in the mode is actually propagating in the cladding.

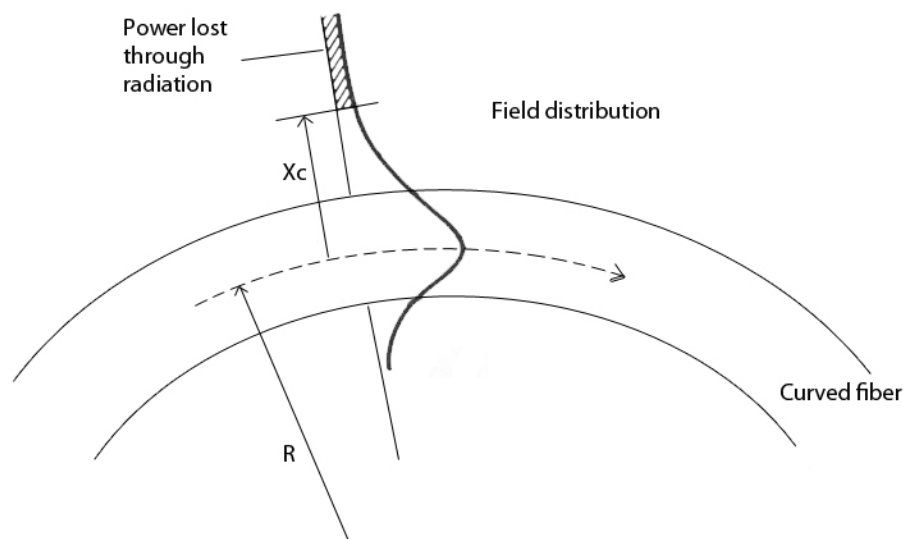


Figure 3.5: Sketch of the fundamental mode field in a curved optical waveguide.

Two primary attenuation factors, dependent upon the external fiber geometry are of interest in this context:

Macrobending losses

If the fiber is curved around a corner, different portions of the same mode must travel at different speeds to maintain the integrity of the mode. However, for portions of the mode traveling through the “outside” of the curve, a small enough radius of curvature will require that this portion of the mode travel essentially faster than light speed. Under these conditions, the mode integrity cannot be maintained and the energy radiates away from the fiber structure, thus contributing to a reduction in the optical power transmitted by the fiber. In general, the amount of attenuation increases exponentially with decreasing radius of curvature. For larger radii, the

losses are typically very small, particularly compared with losses associated with the material phenomena described above. However, beyond a threshold radius, the losses become much larger. Given the increase in modal field intensity distribution near the cladding for higher order propagating modes, macrobending losses are more likely to affect these modes. Thus, a curved fiber typically does not support as many modes as a straight fiber of identical design.

The total number of modes supported in a curved, multimode fiber is therefore related to the index profile, the propagating wavelength, and the radius of curvature:

$$N_{eff} = N_{\infty} \left\{ 1 - \frac{\alpha + 2}{2\alpha\Delta} \left[\frac{2a}{R} + \left(\frac{3}{2n_2kR} \right)^{2/3} \right] \right\} \quad (\text{Equation 3.10})$$

where: N_{∞} = number of modes supported in a straight fiber; α defines the index profile, Δ = core-cladding index difference; n_2 = cladding index, $k = 2\pi/\lambda$; R = radius of curvature of the bend.

Microbending losses

In this case, losses are associated with modal profiles sampling random, microscale fluctuations in fiber radius typically due to nonuniformity in fiber diameter arising during the fiber drawing process or in response to nonuniform radial pressures produced during cabling. **Figure 3.6** depicts this phenomenon. Such microbends are essentially random variation in the fiber geometry (and propagating mode characteristics) along the propagation direction. The result is a coupling between guided wave modes and nonguiding (leaky) modes thus producing an effective loss or attenuation of light within the fiber. Careful packaging (cabling) of fibers and control of draw conditions during fabrication are critical to reducing these effects.

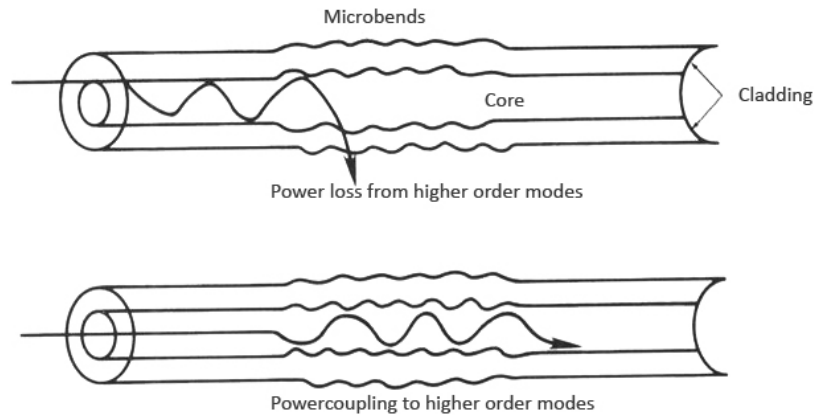


Figure 3.6: Microbending losses arising from small-scale fluctuations in the radius of curvature of the fiber axis.

3.4 Core and Cladding Loss

While earlier discussion focused on light propagation within a homogenous medium, the guiding wave field profile actually intersects both the core and the clad materials comprising the fiber structure. Thus, the overall attenuation observed will reflect this sampling of these two propagation media. For a step index fiber, the effective attenuation will be weighted according to the fraction of the optical power transmitted in each material (i.e. core vs. clad). For the attenuation associated with a mode indices v,m of a step-index fiber:

$$\alpha_{vm} = \alpha_1 \frac{P_{core}}{P} + \alpha_2 \frac{P_{clad}}{P} \quad (\text{Equation 3.11})$$

where: $P_{core,clad}/P$ = the fractional power carried in the core and cladding regions; P = the total power transmitted; $\alpha_{1,2}$ = attenuation coefficients for the core and cladding, respectively.

The total power is then the sum of the fractional powers for each propagating mode. A more complicated relationship, involving the radial behavior of the refractive index, is used for graded index fibers.

Splicing/connection losses

Interconnection of different fiber lengths is a necessary requirement for the assembly of complex fiber transmission and signal manipulation networks. Whether via demountable, physical coupling (via connectorization) or by irreversible splicing techniques (e.g. fusion splicing) alignment of the fiber cores is critical to minimize losses associated with the connection.

In a general sense, successful connections will minimize lateral offset of the core centers, angular misalignment, tilt, and longitudinal displacement (i.e. the formation of a gap). It is also possible that the two fibers to be joined have different absolute core dimensions and varied core-clad diameter ratios as well as different core and cladding glass compositions. **Figures 3.7 and 3.8** are indicative of the type of alignment issues associated with lateral offset and tilt, respectively. Such alignment errors can have a significant effect on fiber coupling efficiency in an optical fiber cable.

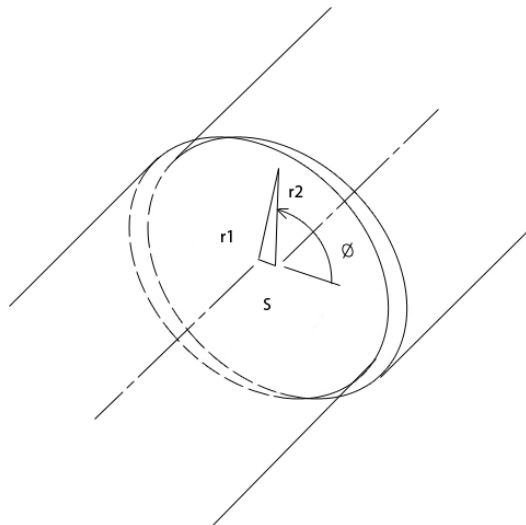


Figure 3.7: *Lateral offset of spliced fibers.*

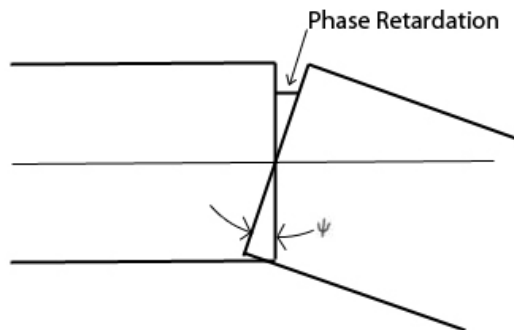


Figure 3.8: *Tilt angle of two spliced fibers.*

Even with perfect alignment and identical fibers to be connected, a typical silica-based fiber core material may have a refractive index of approximately 1.45 at the operational wavelength, producing a reflectivity related loss at the glass-air interface of about 3.5%. For this reason, it is important to eliminate, as much as possible, air gaps in spliced or connectorized fiber cables. Fusion splicing works to replace the interface with a melt-derived boundary between the two fiber segments. The preparation of the fiber ends by appropriate scoring and fracture or by polishing prior to splicing is essential to insure a low loss connection.

In a demountable connector, surface corrosion, contaminant films, and other foreign matter are a constant concern as they will contribute to reflection, absorption and scattering losses at the air interface. While an index matching fluid might be useful to address reflection losses, this is typically not practical. Alternatively, multilayer dielectric anti-reflection coatings can be applied to the fiber ends in order to address reflection concerns. In general, connector designs involving single fibers or multifiber arrays should provide rapid, accurate alignment of fiber ends and longitudinal placement while addressing environmental protection of the fiber ends. Of course, these concerns are heightened for specialty glass fibers utilizing non-oxide glass systems in which environmental tolerances, thermal and mechanical characteristics are even more difficult to address owing to the material's sensitivity to environmental constituents.